Optimal Control of a Reactive Distillation Column

S. Walter

EDRC 06-238-97

Optimal Control of a
Reactive Distillation Column

Stefan Walter

Chemical Engineering Department

Carnegie Mellon University

Pittsburgh, PA 15213

Advisor: L. T. Biegler

November, 1996

Table of contents

i

1. Introduction

In the chemical industry an increasing number of dynamic models of process units or of their combinations is used. The reason is that the steady state is only an ideal condition which is only seldom achieved. In reality the condition of the input streams might vary, e.g. the concentration of the reactants or the pressure of the heating stream changes. The process can be affected by changes inside the unit like poisoning of a catalyst or shrinking of the reaction volume due to sedimentation. Other varying factors are changes in the demand of the products and their specifications. The facts so far affect mainly continuous processes. Discontinuous processes require in general dynamic models for the startup and the shutdown phase. Examples are batch processes which normally are stopped before the steady state is reached.

Today it is often not sufficient to just design a process . It is required that some aspects are optimized besides the profit which is affected by rising costs for heating and cooling. Also the waste production has to be reduced to protect the environment. Another field for optimization is process control. It is too expensive and time consuming to find a good control profile by trial and error in a pilot plant. Also the specifications for products change after increasingly short periods.

Computer models used in the chemical industry often include a large number of variables and equations. It is seldom sufficient to regard the case of ideal behavior of the chemical species to design a unit. A more realistic description of the component properties requires more complex equations with more variables. In many computer models the number of variables for thermodynamic behavior is considerably larger than the rest of the variables. An example is the batch column described in this report. Of the 34 variables per tray are 19 variables are used in thermodynamic relations. The number of thermodynamic variables can be much larger if you use more complex relations instead of the ideal mixture of liquid and vapor phase used here.

Special algorithms are needed to solve these large scale problems in a satisfactory short time. Therefore in this project a reduced SQP algorithm is used for the optimization [1]. It requires less function and gradient evaluations than other methods. Additionally the code takes the almost block diagonal structure of the collocation system into account.

The optimization algorithms for DAE systems can be divided in classes of sequential and simultaneous approach. In the sequential approach the control profiles and the time independent limit are refined by the optimizer. The objective function, constraints and gradient evaluations are calculated using an integrator. The reduced gradients are calculated by sensitivity or adjoint equations. The advantage of this approach lies in the reduced dimensionality of the optimization problem. The integration can be carried out by powerful integrators for a wide class of DAEs. The stepsize is determined internally by the error and stability requirements. The major drawback is that the integration has to be stable and exact for every trial point. Therefore this approach is called a feasible path approach [2].

On the other hand in the simultaneous approach the state and control profiles are discretized. Then the optimization and solution of the system are converged simultaneously. The DAE constraints are discretized as well and the resulting algebraic constraints added to the NLP. Curthell and Biegler applied this idea to examples in chemical engineering, such as reactor design and control [3].

The profiles are discretized by collocation points on finite elements. The advantage of this approach is the treatment of profile constraints as well as the elimination of expensive and possibly infeasible intermediate solutions. The major disadvantage is the size of the problem. It grows dramatically with respect to the size of the original problem. The

1

performance of this algorithm is improved by a reduced-space method exploiting the natural sparsity of the problem due to the collocations on finite elements.

In chapter two the model of the distillation column is described. One section deals with the high index problem. It might arise from careless model formulation. Chapter three explains the advantage of a boundary value formulation of the model. Also the theory behind the integration package COLDAE is outlined. The simultaneous optimization approach is explained in detail in chapter four. A first insight into the processes occurring in the column was obtained by a simple integrator. The results are given in chapter five for different sized columns and different operating policies. Chapter six deals with the results of the different optimization goals like maximum distillate or maximum profit.

2. Distillation model

2.1 Balance equations

The molar holdup and the mole fraction of all components on everyday is calculated as follows:

$$\frac{dB_i}{dt} = M_{+1} \ +L_i\text{-}I \ \text{-}V_, \text{-}L_, \qquad (1.)$$

$$B_i \frac{dx_{i,j}}{dt} = V_{i+1}\left(y_{i+1,j} - x_{i,j}\right) + L_{i-1}\left(x_{i-1,j} - x_{i,j}\right) - V_i\left(y_{i,j} - x_{i,j}\right) + v_j \frac{B_i}{\rho_i} r_i \quad (2.)$$

The reaction has no influence on the molar holdup because the sum of the stoichiometric factors is zero, pi is the molar concentration of the mixture.

The energy balance is given as:

$$^\wedge \ \text{-} \ V \ ^\wedge \ + \ L^\wedge hU + Vft\text{-}^\wedge \ \ + \frac{B_i}{\rho_i} r_i \Delta H_R (\ 3.)$$

Using the expression for the molar holdup (1.) the energy balance can be reformulated in the following way:

$$B_i \frac{dh_i^l}{dt} = V_{i+1}\left(h_{i+1}^v - h_i^l\right) + L_{i-1}\left(h_{i-1}^v - h_i^l\right] - V_i^\wedge \ \ -J_i^l \ +^\wedge \ r_i \Delta H \quad (4.)$$

2.2 Algebraic equations

The equilibrium between the vapor and liquid phase is represented by:

Assuming ideal mixing in the vapor and liquid phase Ki,j can be expressed by:

$$Ki_i \ _{\text{--}W}{}^\wedge; \qquad (6.)$$

The vapor pressure of each component is calculated by the Antoine equation

$$p_j(T) = exp\left(A_j + \frac{B_j}{T}\right)(7.)$$

In a more realistic model of the mixture properties activity coefficients were included. But this model converged only for equimolar feed.

The temperature on every tray is calculated using the fact that the sum of the vapor molfraction equals one.

$$\sum_{j=1}^{} y_j = 1 \qquad (\ldots)$$

Replacing the vapor molfraction by equations (5.) and (6.) you get an implicit function for the temperature.

$$\sum_{j=1}^{nc} p_j\left(T_i\right)x_{i,j} = p_{i,total} \qquad (9.)$$

The liquid flow rates off the trays and the condenser is calculated, as suggested by Gani et al. [4], by:

$$L_i = 999 - [>WQi_{0W})i = K_i(\backslash_w y \qquad (10.)$$

Here it is assumed that the liquid density p is constant. W is the weir length and *how* is the liquid crest over weir. Assuming that the liquid molar concentration *ct* on the trays is constant *how* can be expressed as

$$h_{ow} = \frac{V - V_0}{A} = \frac{B - B_0}{c_t \cdot A} = (B - B_0) \cdot K_2 \qquad (11.)$$

A is the area of the tray, *V* the liquid volume during operation, *Vo* the volume of the tray, *B* the molar holdup during the operation and *Bo* the molar holdup of the tray for the initial feed. Combing equations (10.) and (11.) and replacing the constants by *K* we get the simple expression for the liquid flow rate.

$$L_i = K(B_i - B_{it0})^{2/3} \qquad (12.)$$

2.3   *Index two DAE system and its reformulation*

In the simulation of nonreactive distillation columns it is often assumed that the vapor and liquid flows rates are constant over the whole height of the column. The error of this assumption is only small if the difference in the heat of vaporization of the involved species is only small and the heat loss is neglected. If any exothermic or endothermic reaction takes place on the trays these assumptions don't hold.
In an early version of the computer model I tried to calculate the vapor rate from the energy balance and an algebraic equation for the liquid enthalpy.

The composition is determined by the mass and component balance. The temperature is known from the summation of the vapor composition:

$$\sum_{j=1}^{nc} y_j = \sum_{j=1}^{nc} K_j\left(T_i\right)x_{i,j} = 1 \qquad (13.)$$

The vapor liquid equilibrium is used to calculate the vapor composition and the liquid flow rate from the tray geometry. The specific enthalpies of the vapor and liquid phase are calculated by a thermodynamic function of the composition, pressure and temperature.

$$h_i = f\left(x_{i,j}, T_i, p_i\right) \qquad (14.)$$

3

Thus only the vapor flow rate and the derivative of the liquid enthalpy are unknowns in the energy balance. The vapor rate has to be adjusted in such a way that the value of the integrated energy balance equals the value calculated by the algebraic equation (14.).

$$h_i^l = f\left(x_{i,j}, T_i, p_i\right) = \frac{1}{B_i}\int\left(V_{i+1}\left(h_{i+1}^v - h_i^l\right) + L_{i-1}\left(h_{i-1}^l - h_i^l\right) - V_i\left(h_i^v - h_i^l\right) + \frac{B_i}{\rho_i}r_i\Delta H_R\right)(\ 15.\ )$$

The problem with this formulation of the model is that it has index two. The index of a DAE system is the number of times the algebraic equations have to be differentiated in order to get the first derivative of all variables.

Here the equation of the specific enthalphies has to be differentiated. This combined with the energy balance gives you a new algebraic equations.

$$\frac{df\left(x_{i,j}, T_i, p_i\right)}{dt} = \frac{1}{B_i}\left(V_{i+1}\left(h_{i+1}^v - h_i^l\right) + L_{i-1}\left(h_{i-1}^l - h_i^l\right) - V_i\left(h_i^v - h_i^l\right) + \frac{B_i}{\rho_i}r_i\Delta H_R\right)(\ 16.\ )$$

(16.) has to be differentiated in order to get the first derivative of the vapor flow rates. Therefore the DAE system has the index two.

Thus for a given set of initial values of the differential variables it is not possible to calculate all algebraic variables. Here it was not possible to determine the vapor flow rate. Therefore the derivatives of the differential variables can't be determined, which are vital for the integration forward in time.

The approach to determine the index of the DAE system can be used to reduce the index of the formulation. The equation for the liquid enthalpy (14.) is replaced by (16.). The derivative of the liquid enthalpy df/dt can be expressed as the sum of the partial derivatives with respect to the temperature and the mole fraction of each component.

$$\frac{dh_i^l}{dt} = \frac{df\left(x_{i,j}, T_i, p_i\right)}{dt} \quad \overline{f\,t\,x_{j_i}}\ \ \overline{dt} \quad \overline{\&r_i}\ \overline{dt}^{K}\ (\ 17.\ )$$

The only part of (17.) which is so far unknown is the derivative of the temperature. If the equation for the temperature and the equilibrium relationship are combined and differentiated you get [5]:

$$\frac{d}{dt}\left(\sum_{j=1}^{nc} K_{i,j}x_{i,j}\right) = \sum_{j=1}^{nc} K_{i,j}\frac{dx_{i,j}}{dt} + \left(\sum_{j=1}^{nc} x_{i,j}\frac{dK_{i,j}}{dT_i}\right)\frac{dT_i}{dt} = 0 \quad (\ 18.\ )$$

Thus the derivative of the temperature with respect to time is

$$\frac{dT_i}{dt} = -\frac{\displaystyle\sum_{}^{nc} K \cdot \frac{dx_{i,j}}{}}{\mathrm{fi\_l^*}} \quad \underset{ut_{i,j}}{<} \quad 19\ )$$

$$\sum_{j=1}\mathrm{Yr}_{i,j}$$

Combining (16.), (17.), (19.) and (2.) results in:

$$\frac{1}{B_i} U \left[{}_{+1}\left(h_{i+1}^{v} - h_i^{l}\right) + L_{i-1}\left(h_{i-1}^{l} - h_i^{l}\right) - V_i\left(h_i^{v} - h_i\right) + \frac{B_i}{\tilde{\rho}_i} r_i \Delta H_R \right] =$$

$$\sum_{j=1}^{nc} K_{i,j} dxdt_{i,j} + \left(\sum_{j=1}^{nc} x_{i,j} \frac{dK_{i,j}}{dT_i} \right) - \frac{\sum_{j=1}^{nc} K_{i,j} dxdt_{i,j}}{\sum_{j=1}^{nc} x_{i,j} \cdot \frac{B_{i,j}}{T_i}} \qquad (20.) \text{ where}$$
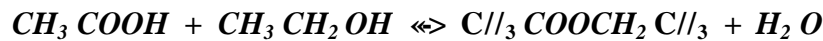
$$dxdt_{i,j} = \frac{1}{B_i}\left(V_{i+1}\left(y_{i+1,j} - x_{i,j}\right) + L_{i-1}\left(x_{i-1,j} - x_{i,j}\right) - V_i\left(y_{i,j} - x_{i,j}\right) + v_j \right| "ij (21.)$$

and

$$\frac{\partial K_{i,j}}{\partial T_i} = \frac{1}{p_{i\,total}} \frac{dp_j(T_i)}{dT_i} = \frac{1}{p_{i\,total}} \frac{-B_j}{T_i^2}\left(\exp\left(A_j + \frac{B_j}{T_i} \right) \right) (22.)$$

This algebraic equation replaces the energy balance. This new formulation has index one.

In this work the reversible reaction of acetic acid and ethanol is used to test the model [6].

$$CH_3\, COOH\ +\ CH_3\, CH_2\, OH\ \ll\gg\ C//_3\, COOCH_2\, C//_3\ +\ H_2\, O$$

$$*_1 = 29000\ \exp\left(-\frac{7150}{T_i}\right) \qquad k_1 = \left[\frac{m^3}{kmol\, min}\right] \qquad (23.)$$

$$*_2 = 7380 \exp(-If>) \qquad k_2 = \left[\frac{m^3}{kmol\, min}\right] \qquad (24.)$$

$$r_{i,j} = v_j \cdot \left(k_{1,i} \cdot c_{alcohol\,i} \cdot c_{acid\,i} \cdots {}^{\wedge}2i \cdot c_{ester\,j} \cdot c_{water\,j} \right) (25.)$$

The expression for the reaction rate is reformulated to use molfraction instead of molar concentration. Assuming ideal behavior of the mixture the overall concentration ct can be expressed as

$$c_{t,i} = \sum_{j=1}^{nc} \rho_j \cdot x_{i,j} \ (26.)$$

The molar concentration of the pure components is assumed to be constant. Using the overall concentration the actual concentration is given as:

$$c_{i,j} = *_{,,;\bullet} \cdot c_{ti} \ (27.)$$

Combining (27.) and (25.) you get

$$r \,.{-}v \cdot (c \ Y\text{-fe} \ \cdot x_{alcohoU} \ {}^{,x_{acidi}} \sim k_{2,i} \cdot {}^{x_{esterj}} \ {}^{,x_{water»}})\qquad\qquad \textbf{(28.)}$$

The complete DAE system is given as:

$$\frac{dx_D}{dt}{}'' = \frac{1}{B_D}\left[V_1\left(y_{i,j}-x_{D,j}\right)+v_j\frac{B_D}{\rho_D}r_D\right]\,(\textbf{29.})$$

$$\frac{dXj}{dt}\sim\frac{1}{B_s}\left[V_{i+1}\left(y_{i+1,j}-x_{i,j}\right)+L_{i-1}\left(x_{i-1,j}-x_{i,j}\right)-V_i\left(y_{i,j}-x_{i,j}\right)+v_{;}\frac{B_i}{Pi}r_{'}\right]\quad(\textbf{30.})$$

$$;i=|2....ntr$$

$$\frac{dx_B}{dt}=\frac{1}{B_B}\left[-V_B\left(y_{B,j}-x_{B,j}\right)+v_j\frac{B_B}{\rho_B}r_B\right]\,(31.J$$

$$\frac{dR_-}{.^\wedge}{-}\mathbf{L},{}^\wedge\,\mathbf{(32.)}\,\,{}^{(R\pm1)}$$

$$\frac{dB_i}{dt}=V_{i+1}+L_{i-1}-V_i-L_i\qquad\qquad ;\bar{i}=1,2....ntr\ \ (\textbf{33.})$$

$$\frac{dB_B}{dt}=L_{ntr}-V_B\ \ (\textbf{34.})$$

where

$$L_i=K\left(B_i-B_{i,0}\right)^{3/2}\qquad\qquad\qquad(\textbf{35.})$$

$$|i=D,|X.\sim ntr$$

$$PtotaU \stackrel{\cdots}{=}\sum_{y\text{-}i}^{nc}p_j(T_i)x_{i,j}=\sum_{j=1}^{nc}\exp\left(A_j+\frac{B_j}{T_i}\right)x_{i,j}\qquad |i=D,|2....ntr,B\ (\textbf{36.})$$

$$y \ -\frac{p_j(T_i)}{Pitotal}\qquad\qquad\qquad ;i=1,2...n»\text{-},fi\ (\textbf{37.})$$

6

$$\frac{1}{B_i}\left(V_{i+1}\left(h^v_{i+1}-h^l_i\right)+L_{i-1}\left(h^l_{i-1}-h^l_i\right)-V_i\left(h^v_i-h^l_i\right)+\frac{B_i}{\rho_i}r_i\Delta H_R\right)=$$

$$\sum_{j=1}^{nc}K_{i,j}dxdt_{i,j}+\left(\sum_{j=1}^{nc}x_{IJ}\frac{dK_{i,j}}{dT_i}\right)-\frac{\displaystyle\sum_{j=1}^{nc}K_{i,j}dxdt_{i,j}}{\displaystyle\sum_{j=1}^{nc}\mathcal{B}_{i,j}}\quad (38.)\ \text{where}$$

$$dxdt_{i,j}=\frac{1}{B_i}\left(V_\wedge\quad_{,j}-x_{i,j}\right)+L_{i-1}\left(x_{i-1,j}-x_{i,j}\right)-V_i\left(y_{i,j}-x_{i,j}\right)+v_j\frac{B_i}{\rho_i}r_i\right)\quad(39.)$$

and

$$\frac{\partial K_{i,j}}{\partial T_i}=\frac{1}{p_{i\,total}}\frac{dp_j(T_i)}{dT_i}=\frac{1}{p_{i\,total}}\frac{-B_j}{T_i^2}\left(\exp\left(A_j+\frac{B_j}{T_i}\right)\right)\quad(40.)$$

The DAE system consists of 30 differential and 31 algebraic equations for a column with four trays, reboiler and condenser and a mixture of four components. The algorithm which is used to solve this system is explained in the next chapter.

3. Solving the model

Ordinary differential equation can be solved by the three following numerical methods [7]:

Single shooting starts from the initial conditions (or the guessed conditions) and solves the DAE system by marching forward in time. In case of a boundary value problem the guessed condition is adjusted by the Newton method in such a way that the boundary conditions are satisfied.

Multiple shooting. In this method the complete integration horizon is divided in several subintervals. On each interval the system equations are solved by a stable integrator. The resulting profiles are combined to find the solution. The continuity between the elements and adjustment of the boundary conditions are enforced by Newton iterations.

Global Method finds the solution simultaneously for the whole horizon (e.g., through orthogonal collocation on finite elements). Therefore no guessing of initial missing conditions is required. In general it is regarded as the most stable method.

Figure 1   Single shooting

Figure 2   Multiple shooting

All methods can be used to solve initial value problems. In order to solve boundary value problems the first two methods have to be modified. In this section the focus will be on the boundary value problems and the modification of single shooting and multiple shooting. In chemical engineering many problems are BVP's, e.g. heat and mass transfer in pipes, mass transfer in catalysts.

In the single shooting method the missing initial condition is guessed and the resulting initial value problem is explicitly integrated. The advantage is that only a small amount of computer memory is required and a small Jacobian matrix has to be inverted for the Newton iteration. Also one can choose between many well implemented integration methods. The major disadvantage is the poor stability for solving boundary value problems containing rapidly growing solution modes. The roundoff error tends to accumulate for unstable DAE systems in a disastrous fashion so that even for good initialization the solution can't be converged.

An attempt to reduce these difficulties is using multiple shooting methods. Here the integration horizon is divided into several subintervals. For BVP's the initial conditions for each element must be given or guessed.

The global method requires the most data storage because all non-zero and fill-ins have to be stored. In contrast SS and MS methods can discard the factorized blocks in the problem and march forward in time.

To illustrate the impact of the boundary conditions and the integration method the following example is considered

$$\dot{z}_2 = \tau^2 z_1 - \left(\pi^2 + \tau^2\right)\sin(\pi t) \quad (41.)$$

$$\dot{z}_1 = \dot{z}_2 \quad (42.)$$

For the initial value problem

$$z_1(0) = 0 \quad (43.)$$

$$z_2(0) = * \quad (44.)$$

the roundoff errors el and e2 in the initial conditions propagate with exponential speed as a function of x and t. Therefore the error is growing dramatically with progress of time even if the roundoff error is very small. If you consider the integration between [0,1] the error at the final time can be written as

$$\varepsilon_{ss}(1) \approx O(\tau \exp(\tau))\|\varepsilon_1, \varepsilon_2\| \quad (45.)$$

For the multi step methods it is assumed that the horizon is divided into N equal spaced intervals. Then the error is given as

$$\varepsilon_{MS}(1) = O\left(\tau \exp\left(\frac{\tau}{N}\right)\right)\|\varepsilon_1, \varepsilon_2\| = \sqrt[N]{\varepsilon_{ss}(1)} \quad (46.)$$

If instead of the initial value formulation the boundary formulation

$$z_1(0) = 0$$

$$z_1(1) = 0 \quad (47.)$$

is used the error can be approximated as

$$\varepsilon_{MS}(1) \approx O(\tau) |\varepsilon_1, \varepsilon_2| \quad (48.)$$

Therefore the boundary formulation is less sensitive to roundoff errors in the boundary conditions.

Only the multi step method can be applied in case of boundary conditions.

A more detailed description of this example can be found in [8].

In an earlier stage of my work I solved the model of the batch column by the IVP package DASSL. By its nature the distillation problem is a initial value problem because all differential variables are given at the starting point. The missing unknowns at the initial point can be determined by solving the algebraic equations.

Starting from this initial point the state variables are approximated as follows

$$z_{i+1} = \beta_{-1} \cdot f(x_{i+1}, z_{i+1}) + \sum_{7=0}^{i} \alpha_j \cdot z_{i-j} \quad (49.)$$

zi are the differential variables, xi the algebraic variables, ocj and j3-l the coefficients determined by the used backward difference method.

DASSL adjusts the stepsize h and the order of the integration method internally controlling the approximation error. Nevertheless the computational time is kept as short as possible. The nonlinear equations in the implicit formulation (49.) are solved by the Newton method. This requires the Jacobian of the differential and algebraic equations. The advantage of the subroutine DASSL is that the Jacobian can be determined internally by finite differences. So the user has the opportunity to concentrate on the programming of the DAE system. The Jacobian is added later when the DAE is implemented correctly. In a more advanced version of the program the Jacobian was specified explicitly. It reduces the computational time required by the finite difference method calculating the Jacobian. Its accuracy was verified comparing it with the results obtained with the finite differences. The Jacobian is essential for the solution of the BVP formulation used for the optimization.

The IVP solver was used to get a general idea of the processes occurring in the column. But in later versions it was replaced by COLDAE because this package can solve BVPs and is more stable than the IVP solver.

COLDAE solves semi-explicit DAE systems of the form [9], [10]

$$f_i(t, z(u), y) \qquad ; i = 1, \ldots, d \quad (50.)$$

$$0 = f_i(t, z(u), y) \qquad ; i = d+1, \ldots, d+m \quad (51.)$$

$$a \leq t \leq b$$

where t is the independent variable, D denotes differentiation of the order mj with respect to t, u and y are the dependent variables, u are the differential and y the algebraic solution components.

For each t

$$z(u) = \left(u_1, Du_1, \ldots D^{m-1}u_1, u_2, \ldots, u_d, Du_d, \ldots, D^{m-1}u_d\right)^T \quad (52.)$$

9

$z(u)$ has $rn^d =]\pounds m$, elements. The system is subject to m side conditions which are given as a nonlinear relationship

$$b_j\left(\beta_j, z\left(u\left(\beta_j\right)\right)\right) = 0 \qquad ; > \cdot -- (53)$$

where $a \wedge P \wedge f \wedge \wedge \ldots \wedge \cdot_m < \pounds$. As special cases this formulation of the side conditions includes initial value and two point boundary value problems.

COLDAE seeks the approximate solution for the differential components ui (t) with piecewise polynomial collocation on a given mesh

$$\pi : a = t_0 \leq t_1 \leq \ldots \leq t_N = b \quad (54.)$$

The k Gaussian collocation points pi $<$ p2 $<$ ... $<$ pk on [0,1] are the zeros of the Legendre polynomial. The collocation points on the mesh elements are then given as

$$t_j = t_{n-1} + \rho_j h_n \quad (55.)$$

The polynomial approximate solution on the finite elements uses a monomial representation. The algebraic solution components are described as

$$u_i^\pi = \sum_{l=0}^{m-1} \frac{(t - t_{n-1})^l}{l!} z_{i,l}(t_{n-1}) + (h_n)^{m_i} \sum_{l=1}^{k} \psi_l \frac{(t - t_{n-1})}{h_n} w_{il} \qquad ; i = 1, 2, \ldots, d \quad (56.)$$

ψ_l are polynomials on [0,1] satisfying

$$D^j \psi_l(0) = 0 \qquad \qquad D^{m_i} \psi_l(\rho_j) = \delta_{jl} \quad (57.)$$
$$; j = 1 \cdot 2 \cdots m \quad i \cdot ,$$

Thus the approximate solution and its first mi -1 derivatives are globally continuous.

The following representation is used for the algebraic solution components yi

$$y_i = \sum \psi_l \frac{(t - t_{n-1})}{h} w_{il} \qquad ; \ i = d + 1, \ldots d+m \quad (58.)$$

The approximate solution has to satisfy the DAE at the collocation points.

$$f\left(t_j, z^\pi(t_j) y^\pi(t_j)\right) \qquad ; i = 1, 2, \ldots, d \quad (59.)$$

$$0 = f\left(t_j, z^\pi(t_j) y^\pi(t_j)\right) \qquad ; i = d+1, \ldots, d+m \quad (60.)$$

Substituting the monomial representations in these equations we obtain (d+m)*k*(N-l) equations. For the continuity requirements you can write (N-l)*m* equations using (56.).

$$\text{"}^{i*}(O = r(zu \ ('\gg \to)) \qquad ; n = 2, \ldots, N ; i = l, \ldots, m^* ; \ 1 = 1, \ldots mj \quad (61.)$$
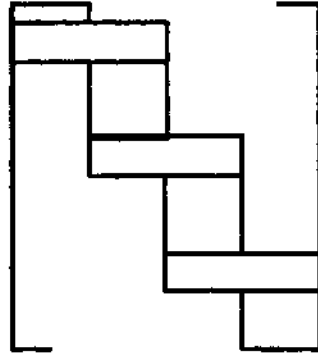
Also the m* side conditions have to be fulfilled. Thus the we have an algebraic, nonlinear system of (d+m)*k*(N-l) + N*m* equations with (d+m)*k*(N-l) + N*m* unknowns.

This system is solved via Newton iterations. We also assume boundary conditions are given only in the form
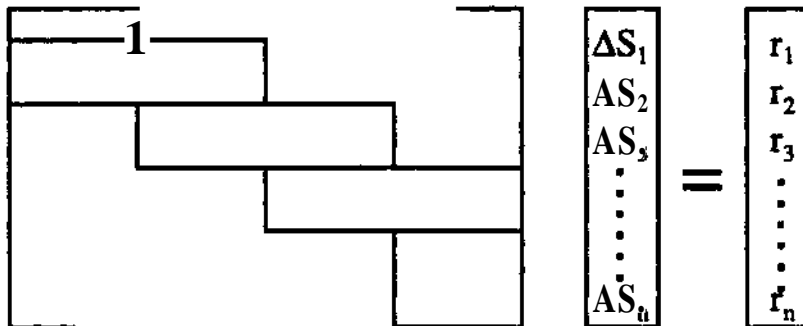
$$B_a\left(u(t_0), y(t_0)\right) = 0$$

$$M«('o)X'o))=o_{(62)}$$

Then the Jacobian is sparse and looks as follows.

Figure 3 Structure of the Jacobian of the collocation system

The square blocks of DAE representation at the collocations points are decomposed reducing the computational costs for the iterations. Thus the following, much smaller system is obtained.

Figure 4   Linear system to determine the next search direction

The iteration ends if the violations are below a user specified limit. By back substitution you get all coefficients for the monomial representation of the approximate solution. They are stored in the vector fspace.

As only first order differential equations are involved in the distillation exapmle I will describe the storing of the solution for this case. The first (N+1) elements of fspace are the mesh points. They are followed by (N+l)*d elements containing the values of the differential variables at the mesh points. The first derivative of the differential variables and the algebraic variables at the N*k collocation points are given in the next (d+m)*k*N elements.

At the end of the calculation all coefficients are given the approximate solution can be calculated by the information of fspace at any point in time using the monomial representation.

11

4. Optimization

After the model is discretized the meshsize has to be fixed. It is obvious that for a very fine mesh the accuracy is very high, while the computational costs increase due to the number of discretized equations. Thus there is a tradeoff between the level of accuracy and problem size. Here five equal spaced interval are used so that the number of discretized elements doesn't get too large.

The optimization problem is solved using a reduced successive quadratic programming (rSQP) method. It is well suited for the solution of large scale process optimization problems with many variables and constraints but only few degrees of freedom. It requires fewer function and gradient evaluations than other methods. As the problem is solved by a simultaneous approach the number of variables and constraints increases with a finer mesh.

In SQP a sequence of search directions is generated by solving a quadratic problem (QP). After this a suitable step size is determined by a linesearch procedure. The QP problem is a local approximation of the NLP by linearizing the constraints. The objective function in the QP is an approximation to the Lagrange function of the problem.

At iteration k the QP subproblem has the following form

$$\min_{nun} \nabla\Phi\left(x^k\right)^T d + \frac{1}{2}d^T B d$$

$$c\left(x^k\right)+\nabla c\left(x^k\right)^T d = 0 \quad (\text{QP1})$$

$$de\backslash c^L-x^k \quad , x^u-x^k]$$

$$x = fe,Ly,u,p,t_f \ J$$

Bk is the Hessian of the Lagrange function at iteration k, c(xk) includes also the inequalities in the NLP. By the introduction of slack variables the inequalities are reformulated as equality constraints.

Since the expected process problems have only few degrees of freedom the computational burden can be reduced further by partitioning the variables into decision variables (control (z)) and dependent (state (y)) variables with a coordinate basis. The dependent variables can be eliminated from the QP along with the equality constraints.

The algorithm used in this work has the following structure

Initialization
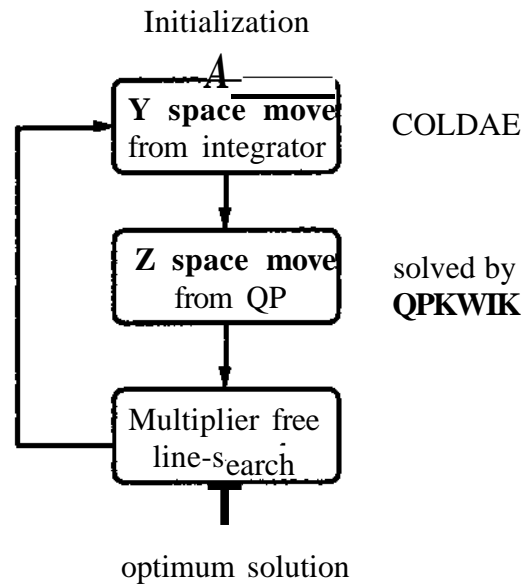
Figure 5   **Algorithm of the reduced SQP method**

Thus the search direction is divided into

$$d=(Yp_y)^k+(Z_{Pt})^k \quad (63.)$$

where Z and Y are defined by

$$Vc^T Z = {}^\wedge 7c_y{}^T \;\; + \mathbf{Vc/]z=0} \quad (64.)$$

We then chose

$$Z =\begin{bmatrix} -\left(\nabla c_y{}^T\right)^{-1} \nabla c_z{}^T \\ I \end{bmatrix} \;;\; Y=\begin{bmatrix} I \\ 0 \end{bmatrix} \quad (65.)$$

with the range space direction (Ypy) obtained by

$$(Vc^r\ Z)>, + (Vc'\ Y)p_y =(Vc'\ Y^\wedge{}_y = \ -\ d(x^k)\{\ 66.)$$

Replacing the search direction d by (63.) you get the new objective function

$$Min Vty^7(x^k) \{ (Yp_y)^t\ (Zp_y)^t \} V \frac{1}{2} (O^\wedge y)^t\ O^\wedge y)^T \wedge (^\wedge Py)^t\ \&>, \} \quad (67.)$$

Taking into account that

$$-p_y=(Vc^r\ Y)^A\ c(x^k) \quad\quad\quad (68.)$$

as a constant, (67) can be reformulated as follows

13

$$Mn \left[\nabla \phi\left(x^k\right)^T Z + Z^T B\left(Y p_y\right)^k \right]_z + \frac{1}{2} p_z^{\ T} Z^T B Z p_z \quad (\text{QP2})$$

$$s.t. \quad x^k \quad + Y p_y + Z p_z e [x^L, x^u]$$

Here ZTBZ is a quasi Newton approximation to the reduced Hessian of the Lagrange function and (ZTBYpy) can be approximated by the Broyden update formula or finite differences.

The Y space move (range space direction) py, including both the collocation and continuity equations, is obtained solving a set of linear equations.

$$-p_y = \left(\nabla c^T Y\right)^{-1} c\left(x^k\right) \quad (69.)$$

As discussed above COLDAE is implemented in the optimization program because it calculates Newton steps for the system of collocation and continuity equations required for the reduced Hessian of the SQP. It exploits the almost block diagonal structure through the use of monomial basis functions and a sparse and stable decomposition.

Moreover, the evaluation of Z can be performed by employing the factorized matrix in COLDAE with different right hand sides This reduces the computational expenses further. As COLDAE is only used to set up and to decompose the system equations in order to obtain a Newton step for fixed elements, the error estimate, the mesh selection and the Newton iteration in the code are suppressed.

After a computer model for the optimizer has been written it is advisable testing it with COLDAE for a given initial condition. At the end of the testing phase you have a converged solution. The profiles of all differential and algebraic variables are stored in the array fspace.

For the optimization the profiles of the variables have to be guesses for an initial condition. The approximated profiles can be found by trial and error. This can be a very time consuming task. In the optimizer the solver of the collocation equations may only use two iterations to find the solution. A better way is using the solution obtained during the testing of the model. COLDAE may use any number of iterations specified by the user. This procedure requires only that COLDAE and the optimizer use the same fixed mesh. During the optimization the solver is given a guess which is fairly close to the real solution. Thus two iterations are sufficient solving the collocation iterations satisfactory. By limiting the number of iterations the computational time is greatly reduced.

If the collocation solver doesn't find the correct solution for the given starting point the wrong search direction is passed to the optimizer. Therefore it may not be able to converge to a solution.

Sometimes it is necessary multiplying the objective function by a factor of one thousand or even bigger. Otherwise the calculated search direction is smaller than the tolerance controlling the progress of the optimization. Then the optimizer stops at the starting point of the optimization with the message that it has reached the optimal point.

5. Test results with the integrator COLDAE

In order to test the model of the batch column the initial feed on every tray was specified as an equimolar mixture of acetic acid, ethanol, water and ethyl acetate. The column consisting of four trays was operated at atmospheric pressure. The temperature in the beginning was the boiling point of the liquid. If not differently stated the holdup of the trays is 1.1 kmole, the holdup of the condenser 2.1 kmole and the bottom contains 10 kmole in the beginning.

The heat was set to 420 kW which corresponds to a vapor rate of approximately 50 kmole/h off every tray at the initial point. The heat input is constant over the regarded time to reduce the complexity of the problem. The column is operated for one hour. The reflux ratio is kept constant at 10000, almost total reflux.

It turned out that after approximately half an hour of total reflux operation the column reached its steady state. The reaction doesn't play a major role in this case due to the slow reaction rate. The boiling points of the pure components are given in the following table.

	Ethanol	Acetic acid	Ethyl Acetate	Water
Boiling temperature for latm [K]	351.44	391.05	350.21	373.15

Table 1   Boiling temperatures of all components
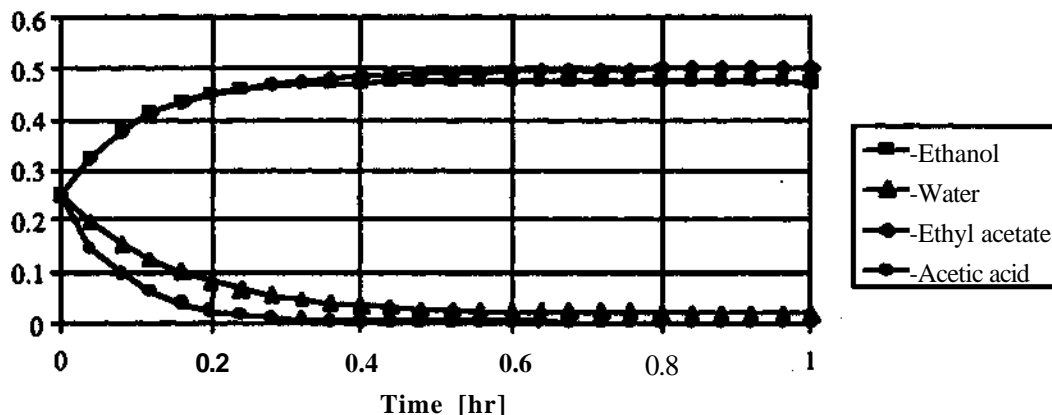
Figure 6 Composition in condenser of 4-tray column versus time

The problem is that the components ethanol and ethyl acetate have both very close, low boiling points. Therefore both accumulate in the condenser while water and acetic acid have the highest concentration in the reboiler. This doesn't improve the conversion of the acid and the alcohol.

Increasing the number of trays doesn't improve the separation of the alcohol and the ester. As an example the composition profile for a column with 15 tray is given. The model which includes four components and a column with 15 trays is the largest simulated problem due to the immense storage requirements of COLDAE. The vector fspace had 8.200.000 elements.
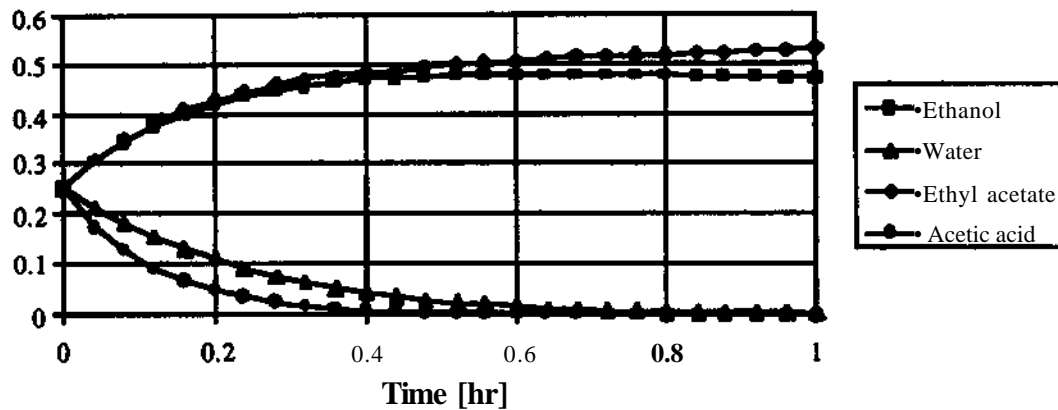
Figure 7   Composition in the condenser of a 15-tray column versus time
This is more obvious if the composition is plotted over the location in the column after one
hour of total reflux operation.
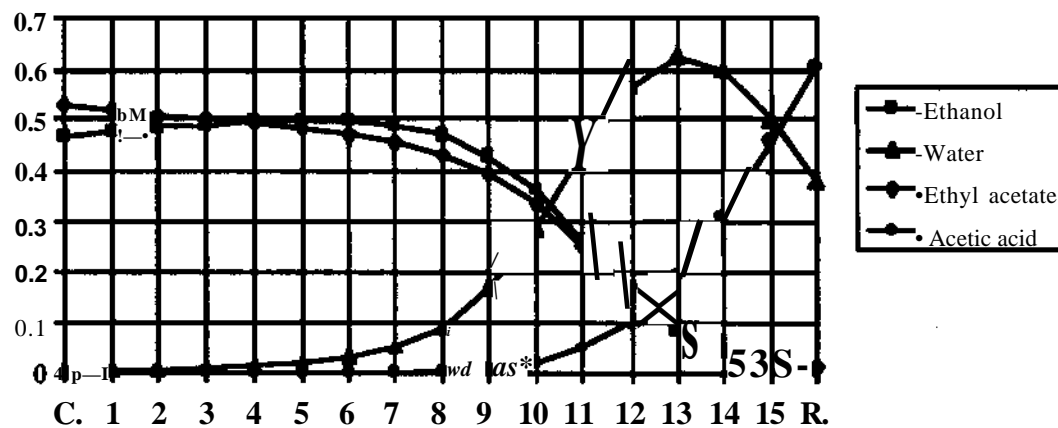
**Figure 8   Composition after one hour of total reflux operation in a column
with 15 tray**

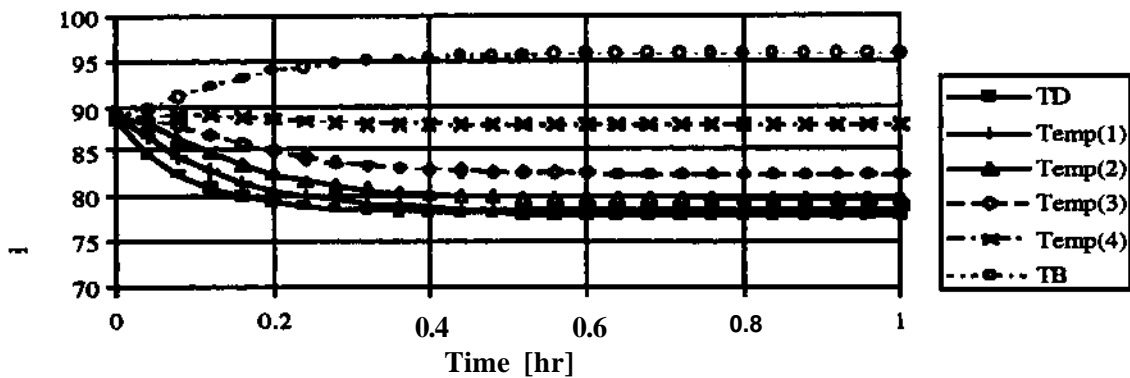As expected the temperature decreases from bottom to the top of the column.

16

Figure 9   Temperature versus time in a column with 4 trays

For the case that the vapor rate is calculated by the energy balance we find that the flows at the top are the lowest and highest leaving the reboiler. This fact can be explained by the differences in the heats of vaporization. Acetic acid and water have the lowest ones and so more moles can be evaporated with a constant amount of heat than in the case of ethanol and ethyl acetate. As the reaction is only slow its heat of reaction doesn't affect the flow rates.

The vapor rates increase for 0.2 hr of *the* total reflux operation because the condenser only takes out the heat of vaporization. This is in beginning smaller than the heat input so that the energy which is used for the vaporization increases.
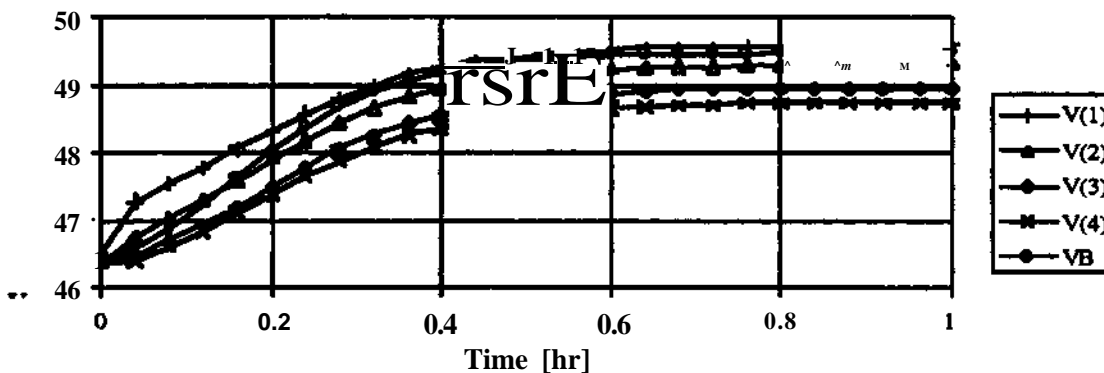
Figure 10   Vapor rates versus time in a column with 4 trays

For the production of ethanol acetate an equimolar feed of ethanol and acetic acid is used. This increases the reaction rate in the beginning of the operation. But after 0.14 hr the reaction has almost stopped.

17
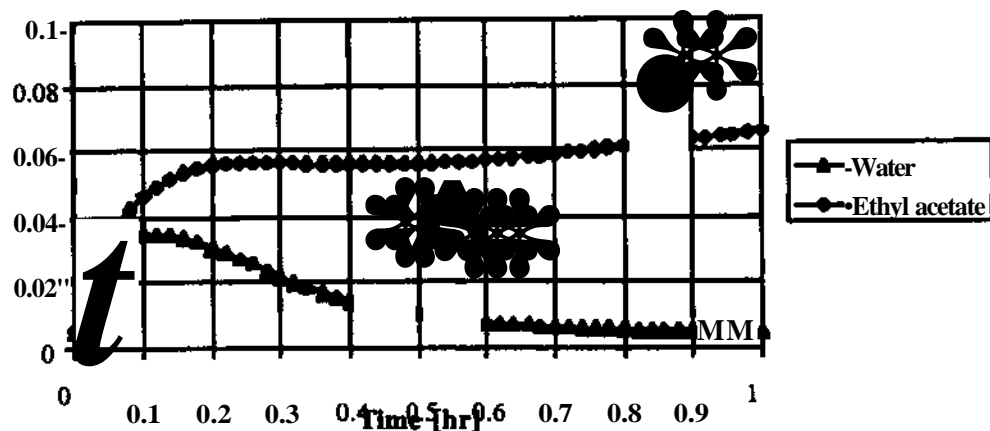
Figure 11 **Water and ester concentration in the condenser for production case**

As the volatility of acetic acid and ethanol is very different the residence time of the acetic acid in the top trays is very short Thus all unreacted ethanol accumulates in the top section of the column while the acid has the highest concentration in the bottom. This results in a low conversion of the alcohol.
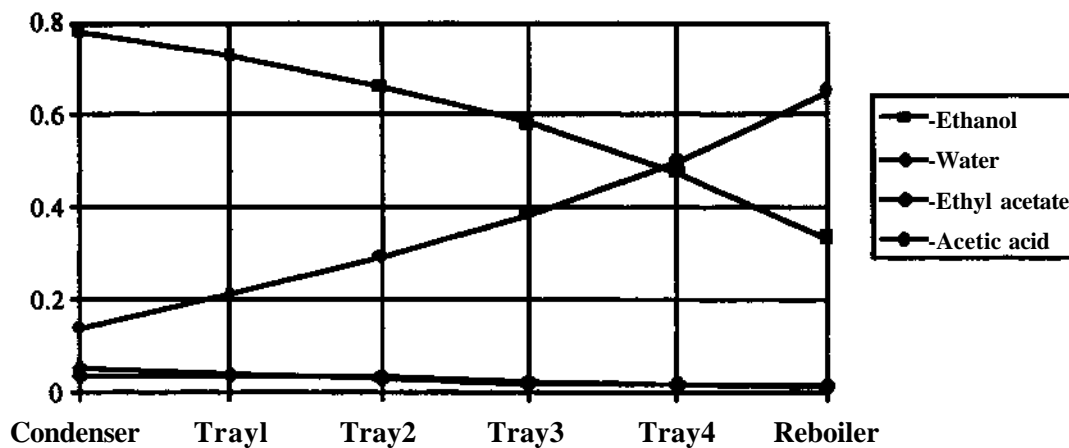

Figure 12 **Composition on trays after one hour for equimolar feed of ethanol and acid**

In order to show the effect of reactive distillation more clearly the reaction rate was increased by the factor 100. Thus for the case of equimolar feed of ethanol and acetic acid the concentration shoots up in the beginning to the high reaction rate. But after a short time the reaction slows down because the reactants are separated in different parts of the column. The increase in ester after 0.1 hours results from the reaction on the other trays and the following separation of the components.

18
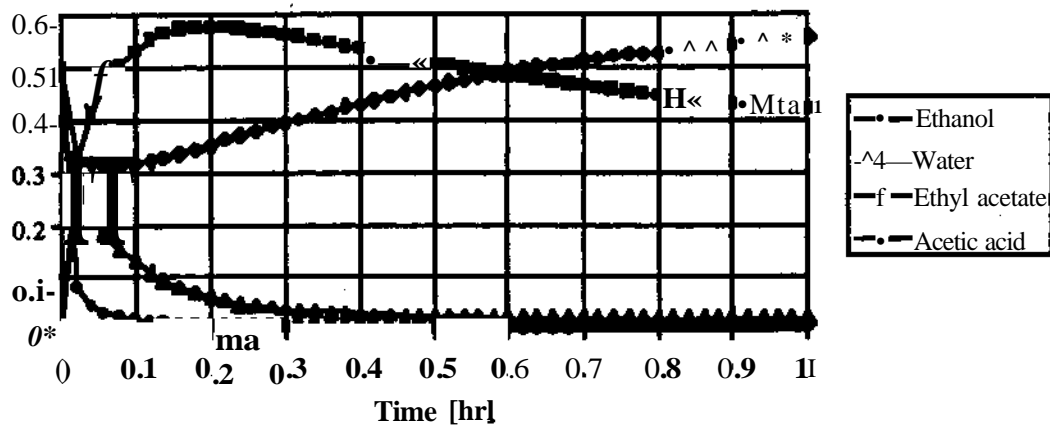
Figure 13   Condenser composition for a 100 fold reaction rate

The initial fast separation is accelerated by the high vapor rates. These result from the heat of reaction. As the heat of vaporization is the same for all trays because initially the composition on all trays is the same. Thus the energy coming from the condensation of the vapor from below is consumed by the vaporization on the tray. The heat of reaction leads to additional vaporization. Thus the initial difference in the vapor rates can be explained.
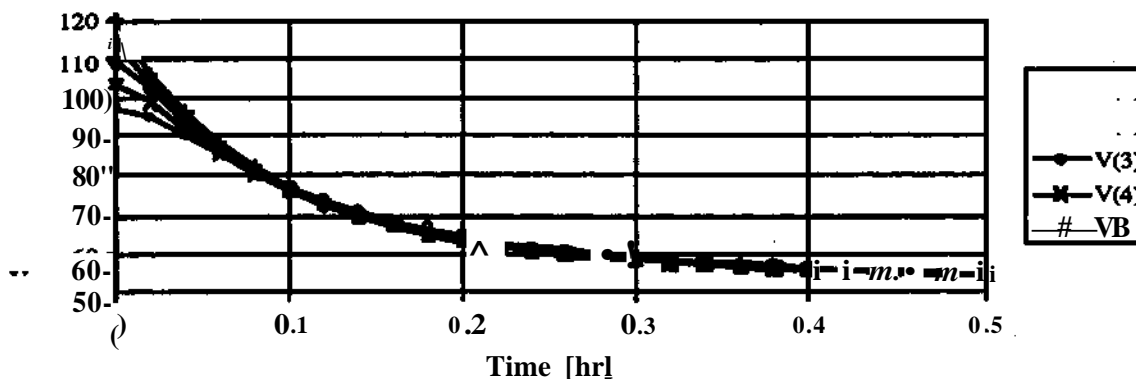

Figure 14   Vapor rates for a 100 fold reaction rate

19

Another production policy starts with pure acetic acid in the column, Ethanol is fed slowly into the reboiler (5 kmole/hr). Thus the composition of the ester is twice as high as in case of equimolar feed of ethanol and acetic acid. But still the concentration of ethanol is very high in the condenser.
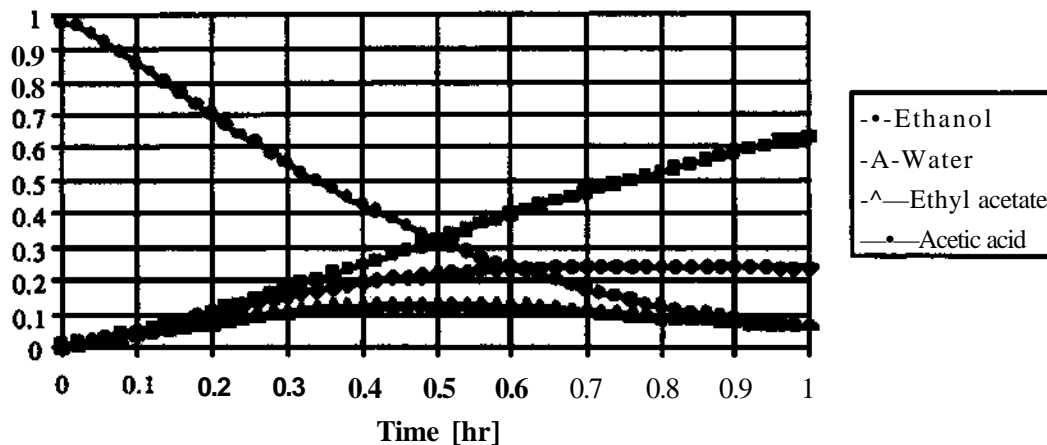
Figure 15 Condenser composition for the case of ethanol feed in the bottom of the column.

After approximately half an hour operation under total reflux condition the column reached its steady state. From this time onward distillate was taken out of the column. The reflux ratio was decreased to 3 and the product composition stayed approximately the same also it didn't meet any concentration which is commercially interesting.
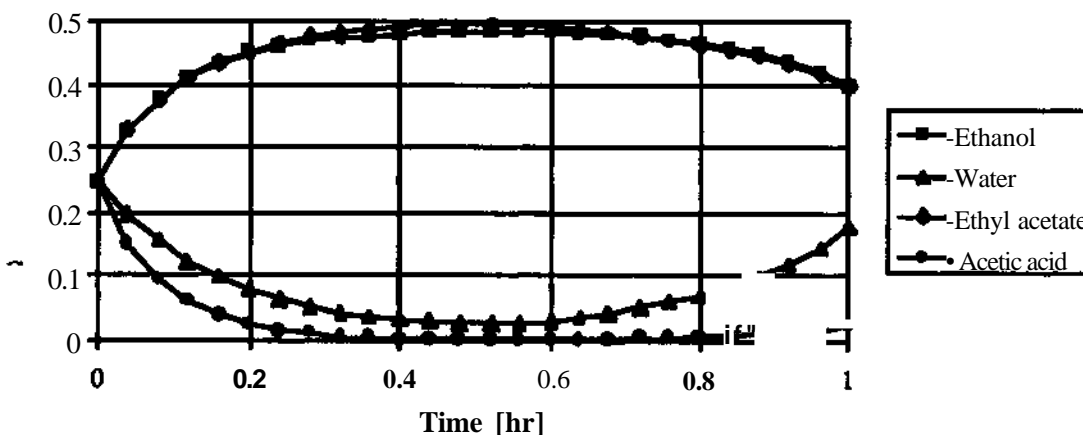
**Figure 16 Composition on trays, reflux ratio = 3 after half an hour**

After 0.4 hours of total reflux operation the temperatures on the trays have reached a steady point. After the reflux ratio is reduced they rise again due to the change of the composition on the trays.

20
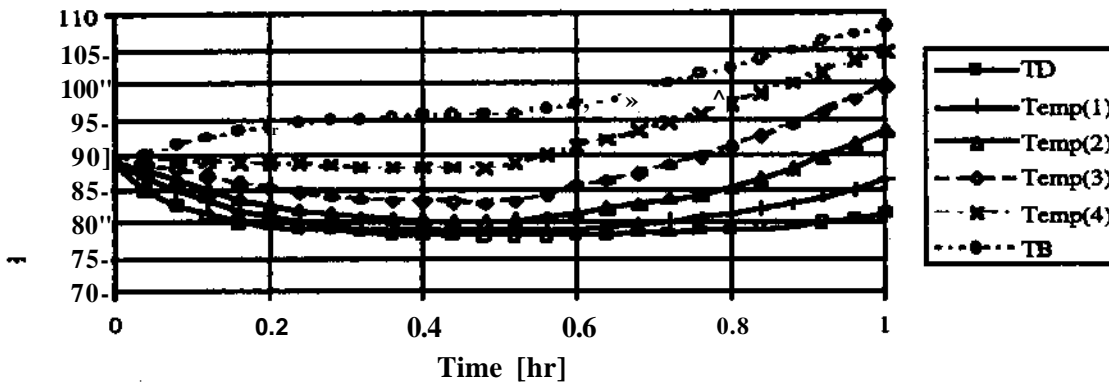
Figure 17 Temperature versus time, reflux ratio = 3 after half an hour

As ethanol and acetic ester are taken out of column the concentration of water and acetic acid increase. As they both have lower boiling points than the other components the temperature rises significantly after the reduction of the reflux ratio.
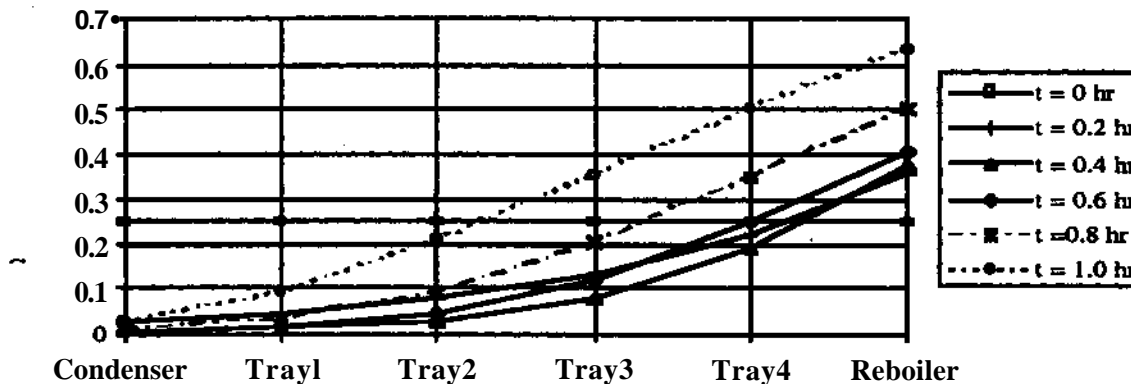
Figure 18 Acetic acid composition versus time

The model was implemented in the SQP optimizer in order to find a more optimal reflux profile. The results are described in the following chapter.

6. Test results of the optimization

For a given column and initial feed the reflux ratio is the only variable, beside the heat input, which can be used as a control for the optimization problem. The disadvantage of the heat input is the delay causes by the heat transfer and the mixing in the reboiler. Also, the range, in which it affects the processes in the column, is much smaller than for the reflux ratio due to the fixed heat exchanger area. Therefore, the heating is not regarded as a possible control variable.

As the heating rate is kept constant the vapor rate is set constant to 50 kmole/h reducing the complexity of the model. This results in a shorter calculation time. Also the required storage is drastically reduced.

21

6.1 *Maximum distillate*

The easiest objective function for the optimization of the batch column is maximizing the amount of distillate produced within one hour. The product has to meet a specified purity constraint, here at least 46% of ethyl acetate in the final distillate. If in the subsequent paragraphs the term 'Ethyl acetate concentration in the distillate' stands for the concentration of Ae ester in the collected overhead product. The column was fed with an equimolar feed of ethanol, acetic acid, ethyl acetate and water.
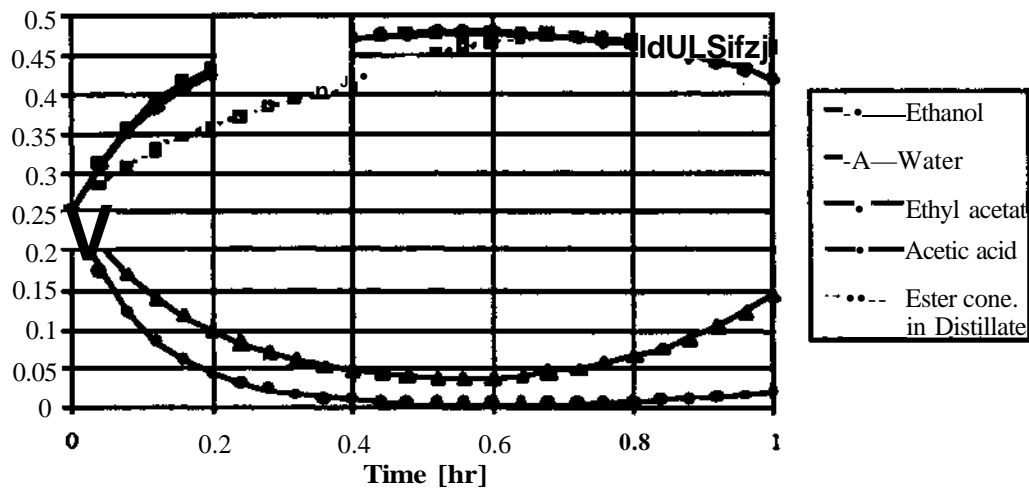
Figure 19   Composition for equimolar feed

The simulation required 51 iterations and took five minutes.The optimizer finds a reflux ratio, which is in the beginning at the upper bound and then drops down to the lower bound. This kind of control profile is called bang-bang control. The reason is, that first the concentration of ethyl acetate is increased by the maximum reflux ratio. At the end the reflux ratio drops to the lower bound taking out of the column as much distillate as possible.

The control profile is not exactly a bang-bang control because a fixed mesh is used for the collocation equations. As explained above, the profile is continuous on each interval. Thus you get the slope between the mesh points 0.4 and 0.6. In order to get a more accurate solution, the mesh points have to be shifted in such a way, that the discontinuity happens at a mesh point.

The kink in the profile of the ethyl acetate concentration in the collected distillate is caused by the change in the reflux ratio. As the reflux ratio goes down, a great stream, purer in ethyl acetate, goes into the distillate collected so far.
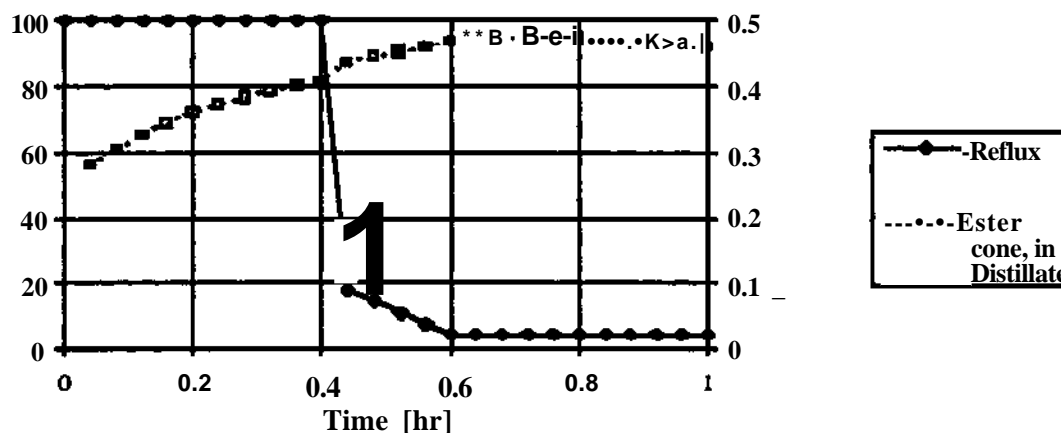

**Figure 20   Reflux ratio for average composition of 46% ethyl acetate**

The reaction rate was accelerated by the factor 100 emphasizing the effect of the reaction during the distillation. An equimolar feed consisting of ethanol, acetic acid, ethyl ester and water was used. Due to the reaction, the composition increases considerably after the reflux ratio has dropped to its lower bound. The change in the reflux ratio can you recognize by the kink in the distillate composition. The concentration of ethanol is lower and the concentration of water increases more towards the end of the operation.
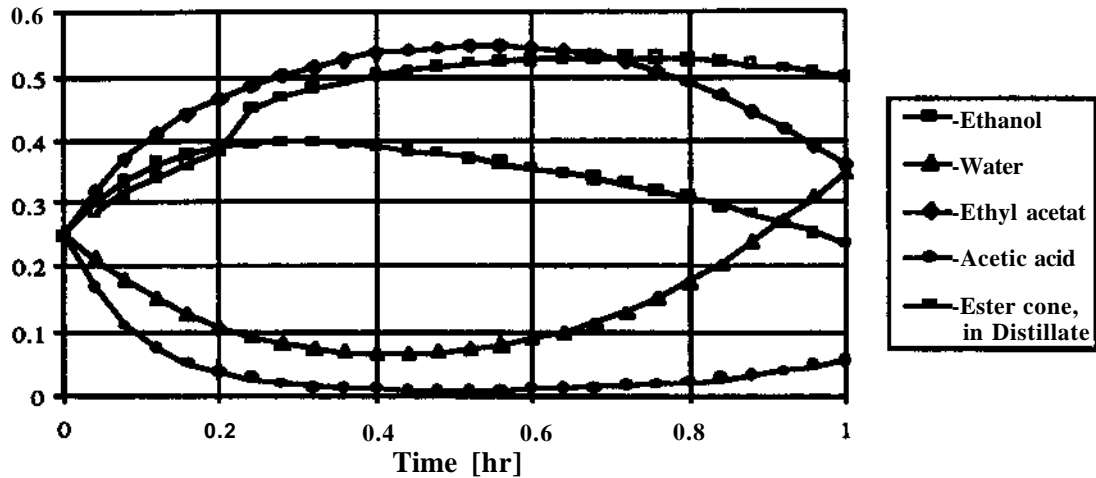
Figure 21   Composition profile in condenser for Max. distillate problem

The example with 50% ethyl acetate in the distillate required 87 iterations and took 8 minutes. As with the slow reaction, the optimal reflux ratio has almost a bang-bang profile. If a purer distillate shall be produced, the switching point appears at a later point in time. For less stringent requirements it is the other way around. Here are the cases of 50% and 55% of ester in the collected distillate considered.

The amount of collected distillate with 55% ester is 5.28 kmole and 7.5 kmole for 50% ester in the overhead product. The reflux ratio stays for a longer time at the upper bound in order to achieve a purer product. But this means that the stream out of the column is small for the same period of time. So only a smaller amount of purer distillate can be produced. This fact can be observed in all the following examples.

24
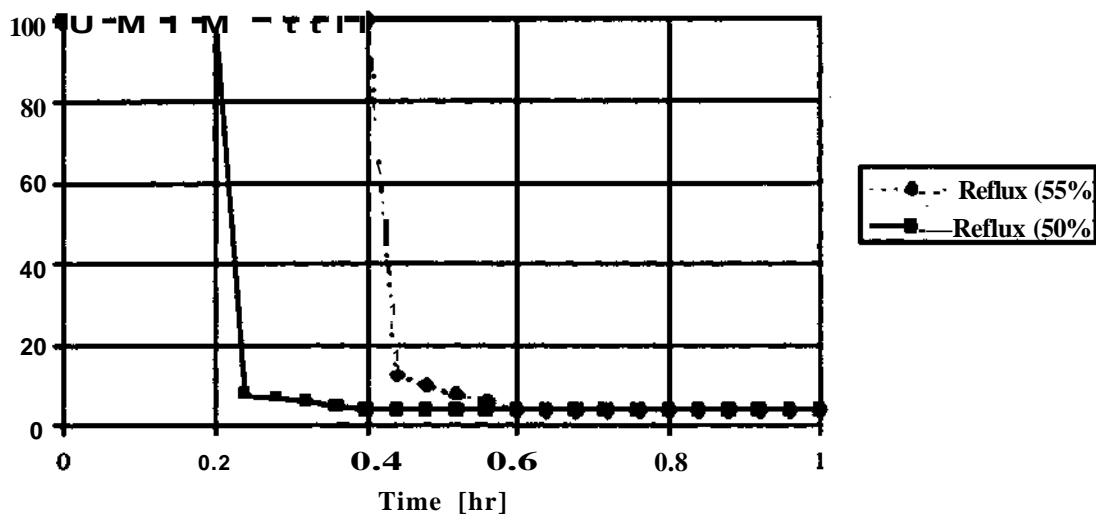
Figure 22   Reflux profiles for different product purities for Max. distillate amount

Another way reducing the complexity of the computer model is considering the reaction in the condenser and reboiler only. Both have considerably larger holdups than the other trays. Therefore, the residence time is longer in them.

Comparing the cases of reaction on the trays and no reaction you see that the profiles of ethanol and ethyl acetate are slightly different. In the case of no reaction on the trays, more ethanol reaches the condenser without being converted to ester. But as the concentration has reached its peak, the reaction rate is higher in the condenser so that in the end the same amount of ester is produced. Despite the differences in the concentration profiles the reflux profiles are equal. Thus, in both cases the same amount of distillate are produced.
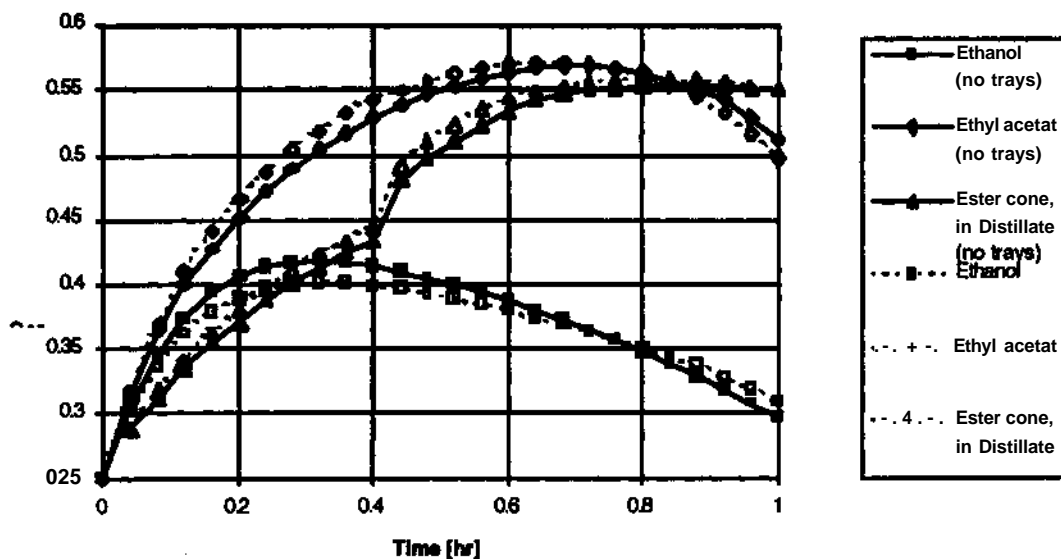
Figure 23   Composition profiles with and without reaction on the trays

In the last case considered for the maximum distillate problem an equimolar feed of ethanol and acetic acid is used. This shall simulate the actual production of ethyl acetate. The real reaction rate is so slow, that no significant processes can be seen. Thus, it is increased one hundredfold. As the computer program has problems beginning with zero concentration of the ester and water, both are added in low concentration (0.5%).

In the beginning, the ethanol concentration increases due to the separation of the alcohol and the acid. After 0.15h, the concentration of ethanol in the condenser goes down steadily as the fast reaction proceeds and the unreacted alcohol is taken out at the top of the column. Again, the optimal reflux policy is the bang-bang control.
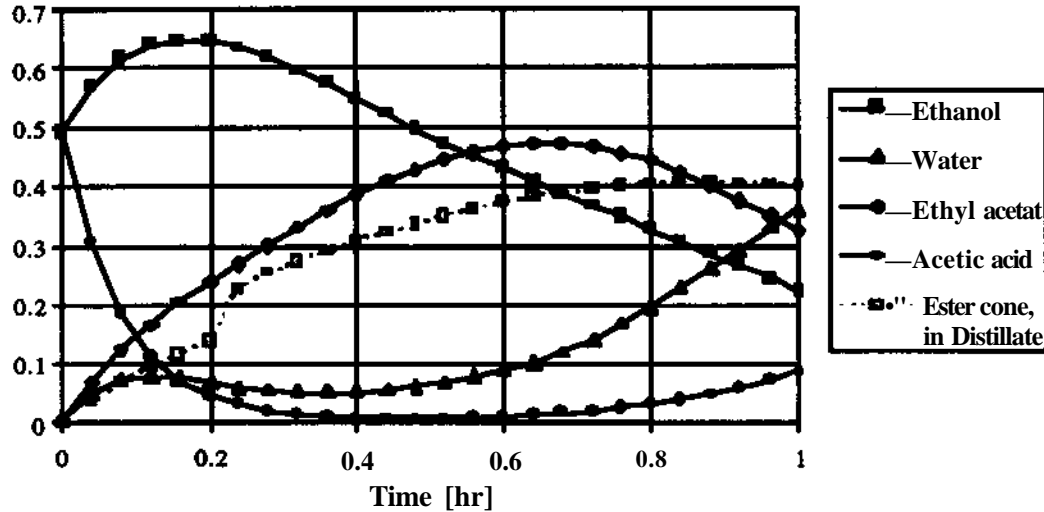

Figure 24   Production of 40% Ester in Distillate

6.2 *Maximum annual profit*

The next used objective function is the maximization of the annual profit As a constant heat input is assumed the heating costs don't affect the objective function.

$$max\frac{profit}{time}=max\frac{price \bullet product\ amount - cost \bullet amount\ educt}{final\ time}$$

The optimizer requires, that a mesh is used on the fixed interval [0,1]. This limitation can be overcome by introducing a variable final time as an additional parameter. All equations containing time as an explicit variable have to be rewritten as follows.

$$t=t_f z_f \qquad ; \quad zx\epsilon\ [0,1]$$

Here only the differential equations are affected.

$$dt = t_f\ dz \quad \Rightarrow \quad \frac{dx}{dt}=\frac{dx}{t_f\ dz}=f(x) \quad \Rightarrow \quad \frac{dx}{dz}=t_f\ f(x)$$

The composition profiles of the components in the condenser are only slightly different from the profiles shown so far. Comparing the results for different costs of the initial feed to the column shows, that the time is increased with rising costs. A greater amount of product is taken out of the column compensating the high costs. For the same purity

26

constraint, the switching point between highest and lowest reflux ratio shifts to an later point for the more expensive feed.

As an example, it is assumed that the costs of the initial feed to the column vary between $0 and $10000 and the price for the product is set to $10000. The results are given in the following table:

Costs for initial feed [$]	0	5000	10000
Operation time [hr]	0.673	0.701	0.729
Overhead product [kmole]	5.17	5.38	5.5

Table 2 Operation time and distillate amount for different feed costs

6.3 *Maximum annual distillate*

The objective function for the annual profit can be simplified by the assumption that the costs for the initial feed are negligible. This can be interpreted as the maximization of the annual distillate production. As an example, the column is filled with an equimolar feed of all four components and the reaction is onehundredfold faster. For different purity constraints on the product it turns out that the operation time has to be increased for a purer product. The reason is that for a purer product a longer total reflux period is required increasing the concentration of the desired component in the condenser. This fact is illustrated in the following figures. The composition of the final product is stated in parentheses.

The slope before the reflux ratio reaches its lower bound is due to the fixed mesh.
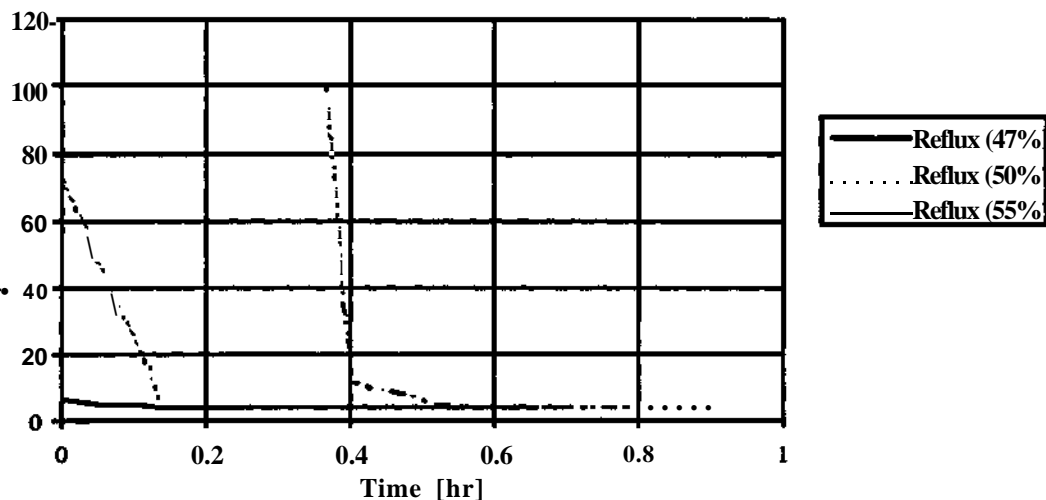
Figure 25   Reflux profiles for different product purities for Max. annual profit problem

The composition profiles show the same trend. The purer the product has to be the more the profile is stretched.

27
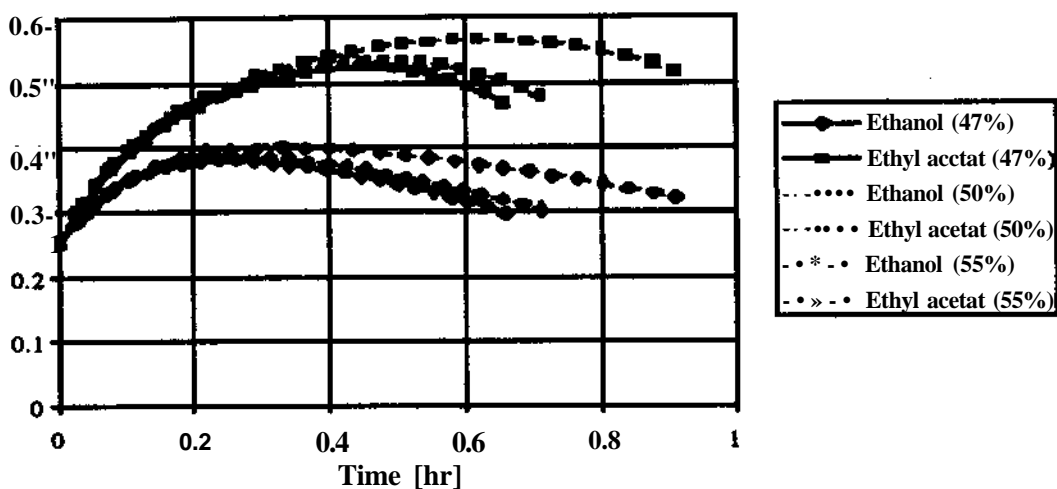
Figure 26   Composition for different product purities for Max. annual profit problem

The simulation for 50% pure product required 18 iterations and two minutes. The example with 55% ethyl acetate in the distillate took 52 iterations and lasted 8 min.

In order to improve the conversion of the reactants, I tried to optimize the reflux ratio and the holdup of the trays. As the holdup is a major design parameter for reactive distillation, it has an important impact on the reflux profile. Increasing the holdup slows down the transient of the concentration profiles. So it takes longer to reach the required purity constraint in the condenser. On the other hand, a longer residence time on the trays increases the conversion of the components. As the esterfication is a reversible reaction, one expects that trays with a high concentration of the reactants have a large holdup while other trays are small resulting in a fast transient of the concentration.

Unfortunately, the reaction is so slow that it doesn't affect the sizing of the trays. The optimizer always choose the lowest holdup to achieve a fast concentration transient. Even for the case of a onehundredfold reaction constant no changes occurred. The separation of the reactants is too fast, so that the reaction dies down.

7.   Conclusions

Future research should include the equations for variable vapor flow rates. As was shown in figure 14 the vapor flow rate off every tray drops down by half after the reaction has died down. The amount of distillate is closely related to the vapor rate. Also it controls the velocity with which the transient of the concentration profiles change. Therefore it has a major impact on the control profile. To illustrate this fact better a reaction is needed in which the reactants accumulate in the same part of the column.

As in all the examples was shown the reflux profile had an almost bang-bang profile. Therefore a variable mesh size and distribution should be incorporated. This way it can be ensured that the discontinuity coincides with a mesh point. This leads to a better solution than determined in the present cases. Another reason for not using an equal spaced mesh is that the concentration on the trays changes significantly in the first fifth of the operation for

the given example. This can be observed very well in the cases where equimolar feed of ethanol and acid are used. (Figure 11)

So far only relative simple objective functions like maximum distillate or maximum annual profit have been considered. A more complex batch operation would involve several product cuts and offcuts. For the here given reaction the mixture of alcohol and ester would be taken out overhead in the beginning. After the ester concentration has dropped to the lower limit the collection of the offcut starts. This operation proceeds until the remaining acetic acid in the column is pure enough for reuse. Concerning the optimizer a different algorithm for the decomposition of the collocation equations is vital.

In the present version of the code an extensive amount of memory is reserved for the storage of intermediate solutions. Thus it is only possible to simulate for a ternary system a column consisting of 15 trays on a HP computer model 712/100. Also changes in the code should improve the speed of the optimization because for example it sometimes took half an hour for a column with 8 trays to reach the optimum. The decomposition is a very time consuming step in the present code.

Like mentioned in Chapter 2 the thermodynamic properties of the mixtures are calculated under the assumption that the vapor and liquid phase behave like ideal mixtures. As the ethanol and the ethyl ester have very close boiling points this is a very risky assumption. Changes in the volatility effect directly the concentration of ethanol in the condenser and therefore in the product Secondly it determines to which extent the alcohol and the acid are converted.

8.   Acknowledgment

9.   References

[1]   Schmid. C; Biegler, L.T.
       Quadratic programming methods for tailored reduced Hessian SQP
       Comput. Chem. Eng.
       Vol. 18, No. 9, pp. 817 - 832, 1993

[2]   Mujtaba, I.M.; Macchietto, S.
       Optimal operation of multicomponent batch distillation -
       multiperiod formulation and solution
       Comput. Chem. Eng.   .   ^/
       Vol. 17, No. 12, pp. 1191, 1993

[3]   Curthell, J.E.; Biegler, L.T.
       Simultaneous optimization and solution methods for batch reactor control profiles
       Comput. Chem. Eng.
       Vol. 13, No. 1/2, pp. 49 - 62, 1989

29

[4]   Gani, R.; Ruiz, C.A.; Cameron, I.T.
        A generalized model for distillaion columns -1
        Comput. Chem. Eng.
        Vol. 10, No. 3, pp. 181 - 198, 1986

[5]   Howard, G.M.
        Unsteady state behavior of multicomponent distillation columns : Part I
        AIChE Journal
        Vol. 16, No. 6, pp. 1022 - 1029, 1970

[6]   Holland, CD.
        Fundamentals of multicomponent distillation
        McGraw Hill, Inc; New York
        1. Edition 1981

[7]   Tanartkit, P.
        Stable Computational procedures for dynamic optimization in process engineering
        Ph.D. Dissertation
        Carnegie Mellon University, Pittsburgh, USA